25th ABCM International Congress of Mechanical Engineering
October 20-25, 2019, Uberlândia, MG, Brazil

COBEM-2019-0670
FLOW-ACCELERATED CORROSION (FAC) – AT LOW-TEMPERATURE AND NEUTRAL WATER

Vagner Silverio
Julio Cézar de Almeida
Department of Mechanical Engineering, Federal University of Paraná, Curitiba, Brazil
vagner.silverio@ufpr.br
j.cezar@ufpr.br

Abstract. *Flow-Accelerated Corrosion (FAC) occurs with a greater susceptibility in carbon steel components that operate at high temperatures. However, the occurrence of FAC at low temperatures and neutral pH has been recorded in cooling and feed systems, with high degradation rates. Thus, the experiment was carried out to collect data for these conditions. Tests were performed in a closed circuit in which the fluid was controlled and monitored while recirculating in the test section. FAC was evaluated using a visual non-destructive test (borescope), micrography, and X-ray Diffraction (XRD).*

Keywords: *Flow-Accelerated Corrosion (FAC), Low-temperature FAC, Flow Loop, and FAC Testing.*

1. INTRODUCTION

Different degradation processes such as erosion, cavitation, corrosion, and others can occur in materials resulting in failure and loss of thickness in tubes/components (Maciejczyk, 2016). As these processes are distinct, in addition to chemical and electrochemical reactions, involving materials dissolved in the fluid itself, the hydrodynamic and physical effects should also be considered characterizing the interactions between the working fluid and the solid wall.

Some forms of generalized corrosion are very common. However, a less familiar form of corrosion is Flow-Accelerated Corrosion (FAC), being according to Trevin (2012), the most worrisome in pipes and equipment of carbon steel that operate in high temperatures, in relation to other materials (Carvalho, 2017).

Damage caused by FAC is usually found between temperatures from 90 to 230 °C. However, component damage at operating temperatures out of this range has already been reported. Over the years, FAC has been reported at low temperatures and in some cases with higher FAC rates than predicted (Dooley et al., 2009; Machiels and Crockett, 2007).

There are reports of low-temperature FAC in which, according to the analysis of the temperature parameter, there would be no great susceptibility to its occurrence (Machiels and Crockett, 2006). Normally, it occurs in the pipeline between the water purification/demineralization process to the point where there is the addition of the pH controlling product (Crockett and Horowitz, 2009). Data on FAC at lower temperatures are rarely found in the literature (Yoneda, Morita, Fujiwara and Inada, 2016).

Therefore, the aim of this study was to increase the understanding of FAC behavior/susceptibility at low temperatures.

2. UNDERSTANDING FLOW-ACCELERATED CORROSION (FAC)

The FAC process consists of two steps, the production of soluble iron at the oxide/fluid interface and the transfer of corrosion products to the bulk flow (Betova, Bojinov and Saario, 2010). Corrosion is controlled exclusively by mass transport (diffusion and convection).

The protective oxide layer (magnetite film) that forms on the inner surface is dissolved, diffusion and dissolution rates are the limiting factors (Fujiwara et al., 2011). High rates of FAC occur in places where there are high rates of mass transfer, corresponding to the turbulent flow of curves, elbows, valves, and others (Mattsson, 2001). At these sites, the protective layer dissolves more quickly, resulting in less protective areas and places with high corrosion rates. This leads to a faster reduction in the thickness of the component.

The water and base material reacts by forming a protective oxide layer on the surface. This oxide dissolves in water forming ferrous ions (Fe^{+2}) and the rate of iron removal (FAC rate) is controlled by the rate of diffusion near the surface. The diffusion depends directly on the concentration of soluble iron ions on the surface of the oxide and the FAC rate depends directly on the increase bulk flow or due to the turbulence (Kain, 2014; Kelley, 2015; Muhammadu, Sheriff and Hamzah, 2013; Song, Jackson, Edmondson and Harrison, 2016).

A second effect of the bulk flow is related to the solubility limit of the soluble ions in the fluid. The solubility limit of ions in a fluid is determined by its specific operating chemistry (temperature and pH).

As the soluble ions reach the flow, the concentration approaches the solubility limit and the dissolution would be reduced if it were a stagnant solution. The bulk flow provides a new solution at the surface, with a great capacity to absorb the soluble ions, thus increasing the rate of corrosion.

The FAC rate depends on the complex interaction of several parameters: fluid characteristics (pH, oxidation potential, the number of phases, dissolved oxygen and others); temperature and kinetics of the chemical reaction; mass transfer or hydrodynamic conditions (bulk flow, geometry, roughness and others); and the chemical composition of the steel (chromium, molybdenum and copper contents).

3. MATERIALS AND METHODS

A wide variety of techniques are available to investigate the FAC. Laboratory techniques used include rotating electrodes; jet impingement; and tubes and channels. For this work, the tests were chosen through tubes and channels. This is because the flow pattern in tubes and channels are similar to those found in plants and are well represented by mass, heat and momentum equations. In the laboratory, tube and channel experiments are usually performed in closed circuits (Schmitt and Bakalli, 2010). Several closed circuits have been developed to investigate how different variables act in the generation of FAC (Ahmed, 2012).

In the closed circuit developed for the tests (Figure 1) around the tube with the external diameter of 1 ½ " (38.10 mm) and a thickness of 3.00 mm was used as a test piece. The test section is designed to reproduce different operating conditions. Thus, it has a length of one meter, ideal to be able to evaluate the effect in the region of entry of the fluid, more susceptible to FAC, as well as the possible occurrence of FAC when the flow is under development and fully developed. The tube used follows the SAE1020 standard.

The structure has the following dimensions: 2.50 m long, 0.63 m wide and 1.50 m high. The test section is positioned in the gray upper part of Fig. 1 and at the end of the test section, on the right side, the inspection window is located.

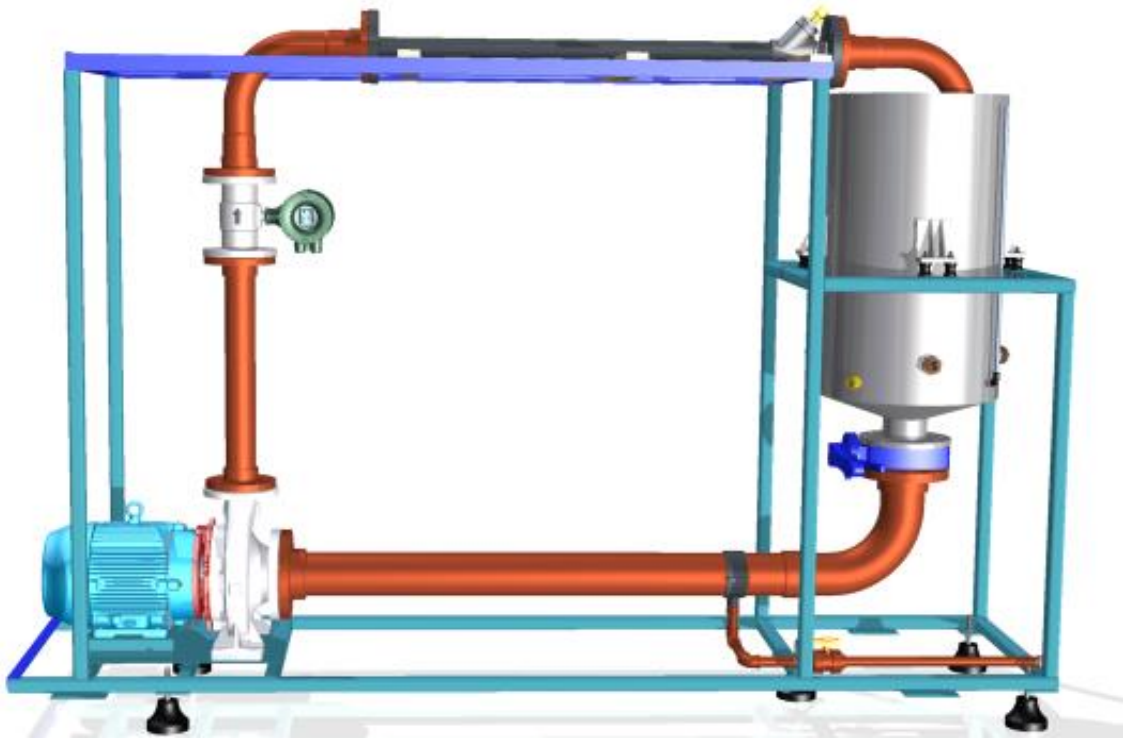

Figure 1. FAC generator system

The selection of materials used in the system as piping, pump, and other components were generally selected to be inert to the experiment. For this reason, materials such as austenitic stainless steel, polyvinyl chloride (PVC), ethylene-propylene-diene (EPDM), natural rubber (NR), Viton® (fluorocarbon rubber) and others are used. Avoiding degradation of the other components during the tests. It should also be concerned with the electrical insulation between materials of different compositions in order to avoid galvanic corrosion.

Data acquisition was performed using LabVEW software, Fig. 2. The fluid and ambient temperatures, the pressure, and the bulk flow were continuously collected during the test. The program also made it possible to check the level of

fluid in the reservoir and remote control of the pump and resistors, as well as the evaluation of the data in real time. The program had an acquisition rate of 100 Hz, averaging those points every second. The program writes the data to an output text file every minute.

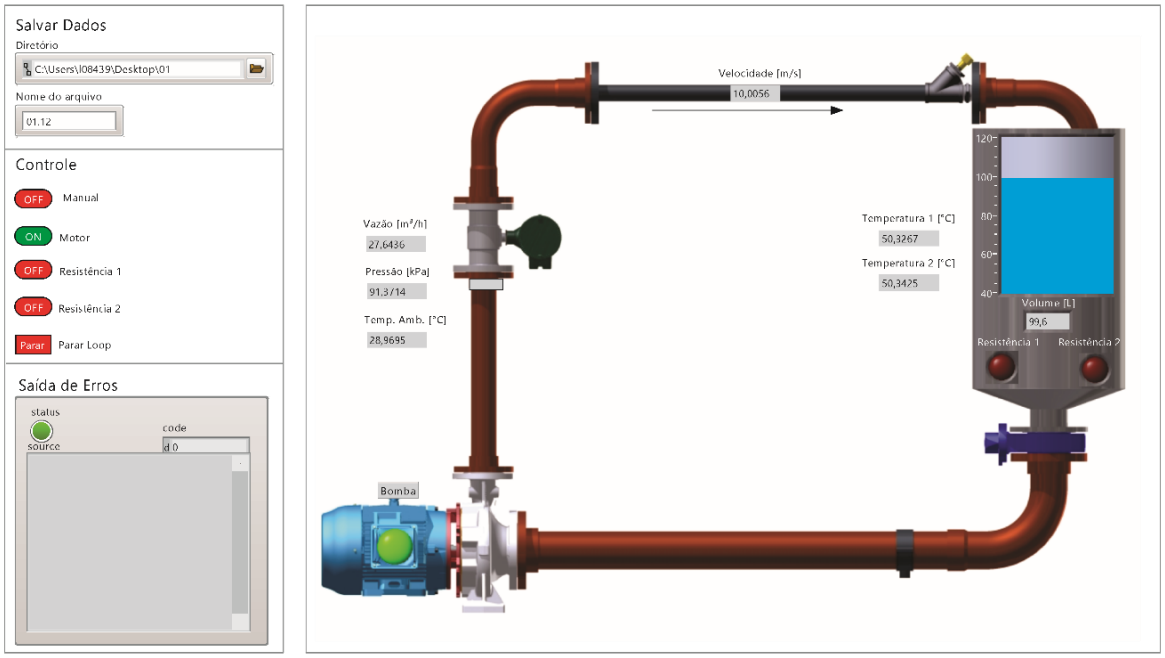

Figure 2 – Interface LabVIEW software

Corrosion monitoring is complex due to the varieties of corrosion applications and parameters (NACE, 1999). Second (NACE, 1999) there is a wide variety of techniques available, but each has its strengths and weaknesses. Thus, it is common to use more than one technique simultaneously so that the negative points of one are compensated for by the positive points of another.

FAC monitoring/analysis was performed by the iron content in the bulk flow, oxidation-reduction potential and a non-destructive test (visual examination - borescope), micrography, Scanning Electron Microscope (SEM), Energy Dispersive X-Ray Spectroscopy (EDS) and X-ray Diffraction (XRD).

The temperature in the FAC has double dependence, of the mass transfer coefficient and the concentration of soluble iron ions (Kain, 2014; Remy and Bouchacourt, 1992; Vepsalainen, 2010). At low temperature is the mass transfer coefficient that has the greatest influence on the FAC. For this reason, was worked different mass transfer coefficients. Industry data suggest that FAC activity begins when flow velocities exceed 5.2 to 6.1 $m \cdot s^{-1}$ (Robinson and Drews, 1999). During the tests, it was detected that the flow above 12.50 $m \cdot s^{-1}$ the fluid began to cavitate in the tube. Therefore, tests were carried out with a velocity of 7.50 to 10.0 $m \cdot s^{-1}$. Three tests were performed at different flow velocities (7.50, 8.75 and 10.00 $m \cdot s^{-1}$), with a duration of approximately 500 hours.

The fluid used had a neutral pH, pH equal to 7.0 ± 0.5, and this variation according to Poulson (2014) does not change the mass transfer conditions since the maximum concentration of iron remains practically the same in the range of pH from 6.0 to 8.0. The temperature used was 50.0 ± 1.0 ° C.

4. RESULTS

4.1 Corrosion morphology

With visual observations made by the borescope, note that at the beginning of the test section there was generalized corrosion and while in the other areas, throughout the test section, there are spot corrosion. These isolated points of corrosion proved to be more severe than generalized corrosion.

4.2 Iron content

During the tests, it was found that the iron ion content during the tests increased at the beginning of the tests and after a certain period, this value decreased. This change in behavior is because iron ions produced by corrosion can dissolve in water and/or deposit on the corroded surface of the metal (Sarin et al., 2004).

4.3 Micrography

The ultrasound technique is usually used to predict the corrosion of components used for longer periods of time (NACE, 1999). however, the ultrasound technique used to measure the oxide layer did not obtain valid results to be presented. This is because the order of magnitude of the uncertainty of the set used - considered in the literature to be half of the wavelength used (Santin, 2003) – be in the same order of magnitude of the necessary measuring range, making the application of the technique/equipment for this work in specific. This is because the test time is relatively small compared to the continuous use of equipment in which the FAC problem occurs. For this reason, it was decided to make the analysis of the FAC by the micrograph technique.

For this analysis, samples obtained from the cross-section of the pipe were used, taking due care that the cut exits perpendicular to the longitudinal direction of the pipe and does not insert errors in the measurement. Prior to the measurement, the sample was stripped according to ASTM G1-03. Measurements of tube wall thickness were performed by the Olympus BX51M microscope, Fig. 3. Fifteen measurements of each tube were made at different points on the untested tube and the test tubes. Subsequently, a comparison was made between the measurements of the untested tube and those tested to evaluate wear.

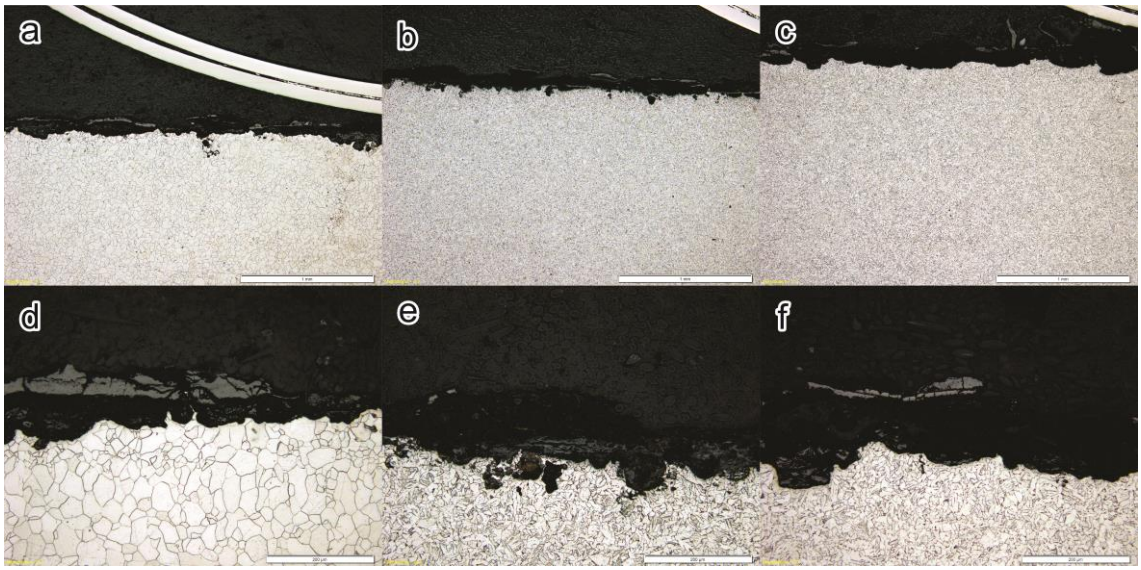

Figure 3. Micrographics – 50x and 200x of magnification
Note: First line 50x magnification and second line magnification 200x; (a) and (d) test velocity of 7.50 $m \cdot s^{-1}$; (b) and (e) test velocity of 8.75 $m \cdot s^{-1}$; (c) and (f) test velocity of 10.00 $m \cdot s^{-1}$.

The average wear sizes obtained for the tests were 38.3 μm, 85.1 μm, and 81.6 μm, respectively for the 7.50, 8.75 and 10.00 $m \cdot s^{-1}$ assays. With the values obtained in the micrography of the thickness reduction and the test time, it was observed that the FAC rates were high (0.67, 1.49 and 1.43 $mm \cdot year^{-1}$). This can lead to premature wear of tubes and components.

4.4 Oxide formed

The analysis of the oxide formed was performed with a Scanning Electron Microscope (SEM), Energy Dispersive X-Ray Spectroscopy (EDS) and X-ray Diffraction (XRD).

Only the results by XRD will be presented, to carry out the test an amount of oxide was removed from the beginning of the test section. The equipment used was the XRD-6000 X-ray diffractometer of Shimadzu.

To identify the present phases, the data-based identification model was used, which compares the data of the obtained diffraction peaks with those of standard samples. The analysis of the material removed from the tubes showed to be a complex mixture of four different phases: magnetite (Fe_3O_4); lepidocrocite (γ-FeOOH); hematite (α-Fe_2O); and goethite (α-FeOOH) (Figure 4).

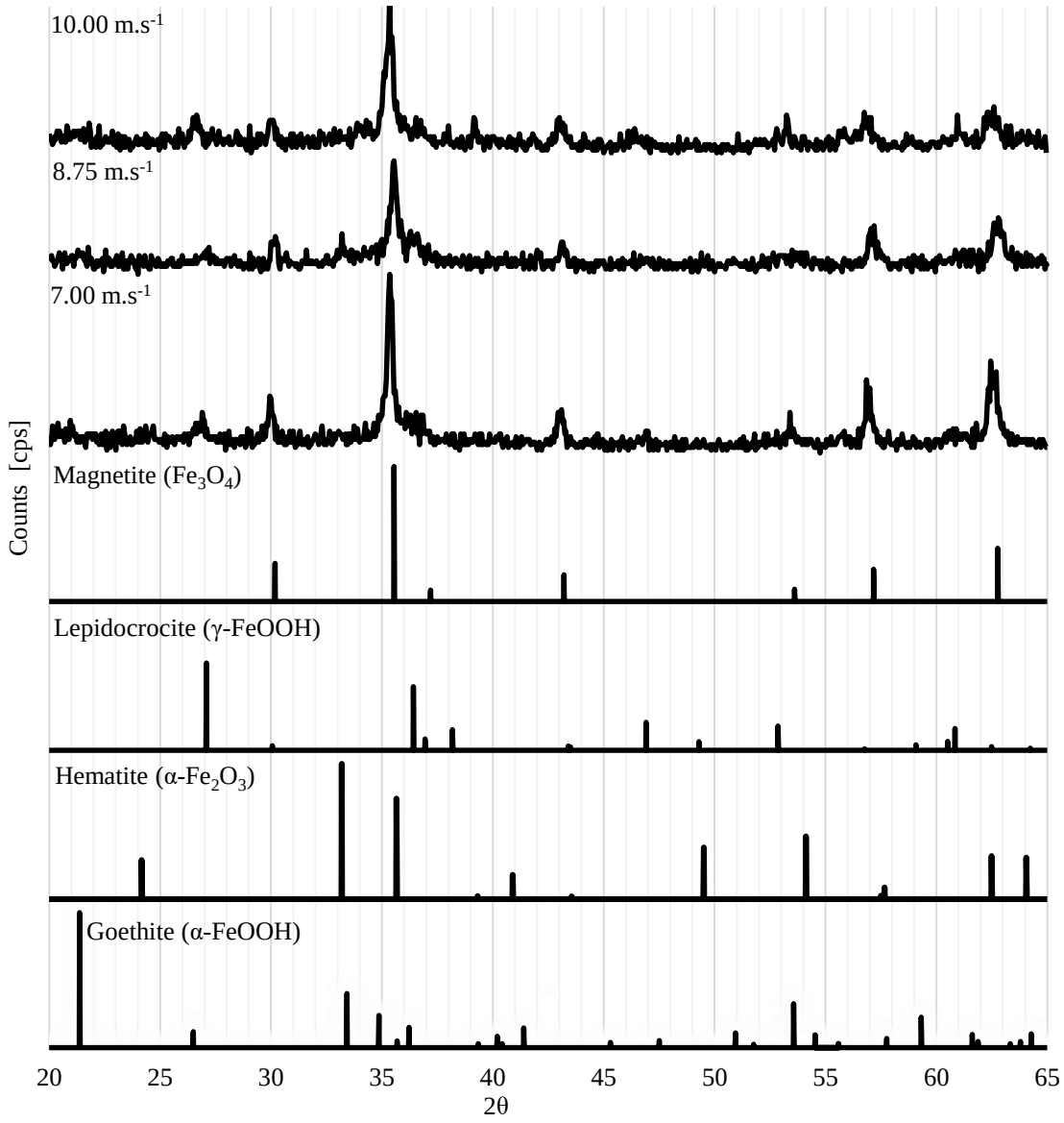

Figure 4. Diffractogram of the tests and standards

5. DISCUSSION

As observed in the experiments, the rate of bulk flow has a great influence on the deposition of iron ions. At a low rate, the deposition may be high as a result of the gravitational force. At the intermediate rate, high static charges between the particulates and the surface can increase deposition. At a high rate, the deposition can be reduced by the shear force of the fluid (Vepsalainen, 2010). This explains the decrease in iron content during the tests and why they occur in different ways. For the intermediate rate test had a higher deposition rate than the lower rate test and the higher rate test in which the deposition was greatly reduced.

As can be seen in the analysis of the oxide formed, it was possible to verify the preferential formation of the magnetite followed by the lepidocrocite and hematite. As proposed the FAC generator system was able to fulfill its purpose and produce the FAC. However, according to Bertrand et al. (2010), at atmospheric pressure and temperatures below 570 °C, only two phases of iron oxides would be stable to magnetite and hematite. Being a thicker layer of magnetite and an outer layer of hematite. The thicker layer of the magnetite is due to the diffusions of the oxygen to the inside and the iron out, so that the layer continues to grow even with the surface covered (Braga, 2009). The hematite layer on the surface of the oxide is due to the oxidation of the magnetite (Betova et al., 2010).

With the analysis of the corrosion by XRD, it was possible to perceive the occurrence of lepidocrocite, which is usually not considered in the literature, because the fluid has a neutral pH. The Lepidocrocite phase is usually found in the internal oxide in tubes and water tanks (Biederman et al., 2008; Chawla, Gurbuxani and Bhagure, 2015; Li, Liu and Chen, 2018). According to Chawla et al. (2015), in wet/aqueous environments the interaction of iron with water the base

material is initially corroded in lepidocrocite, this is consistent with published experimental results. Historical data show that the formation of goethite and lepidocrocite are favored in media with a pH of 5.0 to 7.0, while values of pH, above 8.0 favor the formation of the magnetite. As during the tests the pH was used from 7.0 to 8.0, both phases were formed (Zhou, Zhu and Cai, 2002).

As can be seen in the analysis of the oxide formed, it was possible to verify the preferential formation of the magnetite followed by the lepidocrocite and hematite. As proposed the FAC generator system was able to fulfill its purpose and produce the FAC.

For this work, we focused on the area where the generalized corrosion occurred, as observed by the analyzes performed by the borescope, note that the same occurred at the beginning of the test section exposed to a turbulent flow due to the constriction - reduction of the internal diameter of 60.0 mm for 32.1 mm - which produces high local turbulence.

With increasing shear velocity and stress the oxide layer would become thinner, degrade or would be completely removed (Betova, Bojinov and Saario, 2010), which did not happen according to the means obtained from the micrography.

For this work, we focused on the area where the generalized corrosion occurred, as observed by the analyzes performed by the borescope, note that the same occurred at the beginning of the test section exposed to a turbulent flow due to the constriction - reduction of the internal diameter of 60.0 mm for 32.1 mm - which produces high local turbulence.

With the values obtained in the micrography of the thickness loss and the test time, it was observed that the FAC rates were high (1.88, 2.51 and 2.46 $mm \cdot year^{-1}$). This can lead to rapid tube and component wear and premature failure. With increasing shear velocity and stress the oxide layer would become thinner, degrade or would be completely removed (Betova, Bojinov and Saario, 2010), which did not happen according to the means obtained from the micrography, because the high rate test had a lower wear rate, this should be investigated in future work. The probable cause of this fact is the formation of the laminar sub-layer higher than in the other tests.

6. CONCLUSION

There is a lack of information for the FAC that occurs under normal power plant conditions. To cases identified more recently, such the FAC at low temperatures, the available data is even scarcer. For this reason, further research on the subject is needed. As shown during the experiments it is necessary to better understand the mechanism of the FAC for this condition correlating better the phases formed, the mass transfer rate dependence with the porosity and thickness of the formed oxide, the impact of the iron ions content the mass flow, among other things with the FAC rate. This correlation can be performed through computational simulations, models, genetic algorithms, or others, allowing the development of a system that can be used to predict and mitigate FAC.

7. ACKNOWLEDGMENTS

To Lactec for assigning the use of several types of equipment and the availability of their laboratories for the experimental realization, to the Thermoelectric Plant of Pernambuco (Termope) of the group Neoenergia for the subsidy of the components/equipment purchased for the accomplishment of the tests.

8. REFERENCES

Ahmed, W. H. (2012). Flow Accelerated Corrosion in Nuclear Power Plants. In W. H. Ahmed (Ed.), *Nuclear Power - Practical Aspects* (PP. 153–178). https://doi.org/dx.doi.org/10.5772/51346

Bertrand, N., Desgranges, C., Poquillon, D., Lafont, M. C., & Monceau, D. (2010). Iron oxidation at low temperature (260-500 °c) in air and the effect of water vapor. *Oxidation of Metals*, *73*(1–2), 139–162. https://doi.org/10.1007/s11085-009-9171-0

Betova, I., Bojinov, M., & Saario, T. (2010). Predictive modeling of flow-accelerated corrosion – unresolved problems and issues. *Technical Research Center of Finland (VTT)*, pp. 0–53.

Biederman, J. A., Borch, T., Camper, A. K., Gerlach, R., Butterfield, P. W., & Amonette, J. E. (2008). Evaluation of Characterization Techniques for Iron Pipe Corrosion Products and Iron Oxide Thin Films. *Journal of Environmental Engineering*, *134*(10), 835–844. https://doi.org/10.1061/(asce)0733-9372(2008)134:10(835)

Braga, R. M. (2009). *Medição de camada de óxidos em tubos de superaquecedores de caldeiras aquatubulares por ultrassom*. Universidade Federal do Rio Grande do Sul.

Carvalho, L. (2017). The Facts and a Few Urban Legends Too Around Flow-accelerated Corrosion. *Corrosion*, (9165), 1–7.

Chawla, V., Gurbuxani, P. G., & Bhagure, G. R. (2015). Corrosion of Water Pipes: a Comprehensive Study of Deposits. *Journal of Minerals and Materials Characterization and Engineering*, *11*(05), 479–492.

https://doi.org/10.4236/jmmce.2012.115034

Crockett, H. M., & Horowitz, J. S. (2009, July). " LOW TEMPERATURE" FAC. *ASME*, (PVP2009-78029), 1–10.

Dooley, R. B., Shields, K. J., Shulder, S. J., Howell, A. K., Aspden, J. D., DuPreez, F., & Mathews, J. A. (2009, June). EPRI's Guideline on Chemistry for Fossil Units with Air-cooled Condensers (ACCs). *EPRI*, 1–16.

Fujiwara, K., Domae, M., Yoneda, K., Inada, F., Ohira, T., & Hisamune, K. (2011). Correlation of flow accelerated corrosion rate with iron solubility. *Nuclear Engineering and Design*, *241*(11), 4482–4486. https://doi.org/10.1016/j.nucengdes.2011.04.035

Kain, V. (2014). Flow accelerated corrosion: Forms, mechanisms and case studies. *Procedia Engineering*, *86*, 576–588. https://doi.org/10.1016/j.proeng.2014.11.083

Kelley, A. D. (2015). Flow Accelerated Corrosion – Detection and Mitigation. *Corrosion*, (5574), 1–7.

Li, M., Liu, Z., & Chen, Y. (2018). Physico-chemical characteristics of corrosion scales from different pipes in drinking water distribution systems. *Water (Switzerland)*, *10*(7), 19–21. https://doi.org/10.3390/w10070931

Machiels, A., & Crockett, H. (2006). Investigation into Flow-Accelerated Corrosion at Low Temperatures. *EPRI*, (1013474), 1–84.

Machiels, A., & Crockett, H. (2007, November). Investigation into Flow-Accelerated Corrosion at Low Temperatures. *EPRI*, (1015170), 1–102.

Maciejczyk, J. (2016, February). IDEA's 29th Campus Energy Conference. *Boiler Tubing Failure Reduction*, 1–22.

Mattsson, E. (2001). Basic Corrosion Technology for Scientists and Engineers. In *The Institute of Materials* (Segunda). Retrieved from http://books.google.com/books?id=l9JRAAAAMAAJ&pgis=1

Muhammadu, M., Sheriff, J., & Hamzah, E. (2013). A Review of Literature for the Flow Accelerated Corrosion of Mitred Bends. *International Journal of Emerging Technology and Advanced Engineering*, *3*(8), 663–677.

NACE. (1999). Techniques for Monitoring Corrosion and Related Parameters in Field Applications. *Report*, *Dezembro*(24203), 41.

Pietralik, J. M. (2012). The Role of Flow in Flow-Accelerated Corrosion under Nuclear Power Plant Conditions. *E-Journal of Advanced Maintenance*, *4*(2), 63–78.

Poulson, B. (2014). Predicting and Preventing Flow Accelerated Corrosion in Nuclear Power Plant. *International Journal of Nuclear Energy*, *Outubro*, 1–23. https://doi.org/10.1155/2014/423295

Remy, F. N., & Bouchacourt, M. (1992). Flow-assisted corrosion: a method to avoid damage. *Nuclear Engineering and Design*, *133*(1), 23–30. https://doi.org/10.1016/0029-5493(92)90084-9

Robinson, J. O., & Drews, T. (1999). Resolving Flow-Accelerated Corrosion Problems in the Industrial Steam Plant. *Corrosion*, (346), 1–7.

Santin, J. L. (2003). *Ultra-som - técnica e aplicação* (Segunda). Curitiba, PR.

Sarin, P., Snoeyink, V. L., Lytle, D. A., & Kriven, W. M. (2004). Iron Corrosion Scales: Model for Scale Growth, Iron Release, and Colored Water Formation. *Journal of Environmental Engineering*, *130*(4), 364–373. https://doi.org/10.1061/(ASCE)0733-9372(2004)130:4(364)

Schmitt, H. G., & Bakalli, M. (2010). Flow assisted corrosion. *Shreir's Corrosion*, (m), 954–987. https://doi.org/10.1016/B978-044452787-5.00039-1

Song, F., Jackson, J., Edmondson, J., & Harrison, J. (2016). Flow Accelerated Corrosion of Carbon Steel Pipe Carrying Hot Condensate Water in a Chemical Plant. *Corrosion*, (7127), 1–14.

Trevin, S. (2012). Flow accelerated corrosion (FAC) in nuclear power plant components. In *Nuclear Corrosion Science and Engineering* (pp. 186–229). https://doi.org/10.1533/9780857095343.2.186

Vepsalainen, M. (2010). Deposit formation in PWR steam generators. *VTT Technical Research Centre of Finland*, *VTT-R-0013*, 1–33.

Yoneda, K., Morita, R., Fujiwara, K., & Inada, F. (2016). Development of flow-accelerated corrosion prediction method (1) Acquisition of basic experimental data including low temperature condition. *Mechanical Engineering Journal - JSME*, *3*(1), 1–15. https://doi.org/10.1299/mej.15-00232

Zhou, H., Zhu, H., & Cai, L. (2002). Corrosion inhibition of silicate in the desalination cleaning solution for iron antiques. *Sciences of Conservation and Archaeology*, *14*, 51–62.

9. RESPONSIBILITY NOTICE

The authors are the only responsible for the printed material included in this paper.